

Quantum-inspired optimization for wavelength assignment

Aleksey S. Boev,¹ Sergey R. Usmanov,¹ Alexander M. Semenov,¹ Maria M. Ushakova,¹
Gleb V. Salahov,¹ Alena S. Mastiukova,¹ Evgeniy O. Kiktenko,¹ and Aleksey K. Fedorov¹

¹*Russian Quantum Center, Skolkovo, Moscow 143025, Russia*

Problems related to wavelength assignment (WA) in optical communications networks involve allocating transmission wavelengths for known transmission paths between nodes that minimize a certain objective function, for example, the total number of wavelengths. Playing a central role in modern telecommunications, this problem belongs to NP-complete class for a general case, so that obtaining optimal solutions for industry relevant cases is exponentially hard. In this work, we propose and develop a quantum-inspired algorithm for solving the wavelength assignment problem. We propose an advanced embedding procedure for this problem into the quadratic unconstrained binary optimization (QUBO) form having an improvement in the number of iterations with price-to-pay being a slight increase in the number of variables (“spins”). Then we compare a quantum-inspired technique for solving the corresponding QUBO form against classical heuristic and industrial combinatorial solvers. The obtained numerical results indicate on an advantage of the quantum-inspired approach in a substantial number of test cases against the industrial combinatorial solver that works in the standard setting. Our results pave the way to the use of quantum-inspired algorithms for practical problems in telecommunications and open a perspective for the further analysis of the employ of quantum computing devices.

I. INTRODUCTION

Optimization is a tool with applications across various technologies [1]. However, solving complex real-world optimization problems is computationally intensive even in the case of using advanced, specialized hardware. Quantum computers are widely believed to be useful for solving computationally difficult optimization problems beyond the capability of existing computing devices is to use quantum optimization [2–6]. A general approach consists in encoding a cost function in a quantum Hamiltonian [7], so that its low-energy state is obtained starting from a generic initial state. Among existing methods to achieve such dynamics, quantum annealing offers physical implementations of a non-trivial size [8]. Quantum annealing is by now explored for analysis of various areas, such as chemistry calculations [9, 10], lattice protein folding [11, 12], genome assembly [13, 14], solving polynomial systems of equations for engineering applications [15] and linear equations for regression [15], portfolio optimization [16–19], forecasting crashes [20], finding optimal trading trajectories [21], optimal arbitrage opportunities [22], optimal feature selection in credit scoring [23], foreign exchange reserves management [24], traffic optimization [25–27], scheduling [28–33], railway conflict management [32, 33], and many others [5]. Advances also include the recent experimental demonstration of a superlinear quantum speedup in finding exact solutions for the hardest maximum independent set graphs [34].

Although quantum optimization algorithms suggest an intriguing possibility to solve computationally difficult problems beyond the capability of classical computers, exiting conceptual and technical limitations make it challenging to use it for solving problems of industry relevant sizes. Attempts to simulate quantum computations classically resulted in a new class of algorithms and techniques know as *quantum-inspired* [35, 36].

As soon as these algorithms are compatible with currently existing (classical) hardware, analyzing their limiting capabilities and advantages over classical approaches are required towards their use in practice. Specifically, a way to solve combinatorial optimization problems via simulating the coherent Ising machine (SimCIM) has been proposed [35]. SimCIM algorithm is able to solve optimization problems that are formulated in the quadratic unconstrained binary optimization (QUBO) / Ising form, which can be done for various practically relevant cases [7]. The SimCIM approach has demonstrated capabilities to outperform *bona fide* coherent Ising machine and existing classical methods for certain GSet graphs. However, one of the arising questions is related to the need in to tune hyperparameters [35]. For a wide range of benchmark of quantum-inspired heuristic solvers for quadratic unconstrained binary optimization, namely D-Wave Hybrid Solver Service, Toshiba Simulated Bifurcation Machine, Fujitsu Digital Annealer, and simulated annealing on a personal computer, see also Ref. [37].

Design of optical communication network is a specific industrial avenue, in which combinatorial optimisation is ubiquitous. Examples of tasks include finding optimal transmission and reservation paths, frequency allocation, network throughput maximization and many others [38, 39]. A notable example is the routing and wavelength assignment (RWA) problem, which consists in allocating transmission wavelengths and finding transmission paths between nodes that minimize the total number of wavelengths. Conventional techniques, such as linear programming and mixed integer programming, are useful for most of the cases; however, the combinatorial nature and hardness of the problems make it extremely challenging to apply these techniques for large-scale problems. It is then reasonable to assume that telecommunication industry may benefit from the use of quantum-inspired algorithm in the near-term horizon and quantum com-

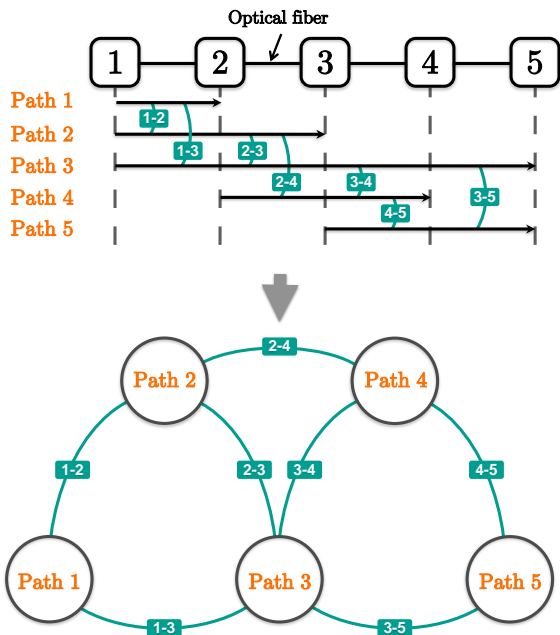


FIG. 1. Illustration of the approach. A linear network with generated requests and paths consisting of 5 nodes, 4 edges, and 5 traffic paths is considered: Solid lines represent original edges, and the arrows lines represent traffic paths. One can reduce the WA problem to a graph coloring problem with a simple graph transformation (bottom of the figure): Each traffic path is now considered a vertex; if two traffic paths share (at least) one fiber they are connected by an edge.

puting in the future [40, 41].

In this study, we consider the variant of the RWA problem. To explain more precisely, we focus on the wavelength assignment task for known routes which we further refer to as the wavelength assignment (WA) problem. This problem is generally NP-hard, so its solution is computationally challenging for large sizes. We propose an original way to transform the WA problem to the QUBO form, which makes it compatible with quantum-inspired optimization algorithm and, in principle, quantum annealing hardware. For solving this problem, we develop a technique based on the SimCIM quantum-inspired optimization solver [35] with the use of the Lagrange multipliers for minimizing the number of hyperparameters. Our numerical results indicate on an advantage of the quantum-inspired solver in a number of test cases against the industrial combinatorial solver working on the standard settings.

II. WAVELENGTH ASSIGNMENT PROBLEM (WA)

Let us consider a network connecting a number of endpoints with optical links (see an example in Fig. 1.) Several endpoints that are interconnected by optical links sequentially comprise a path between transmitter and

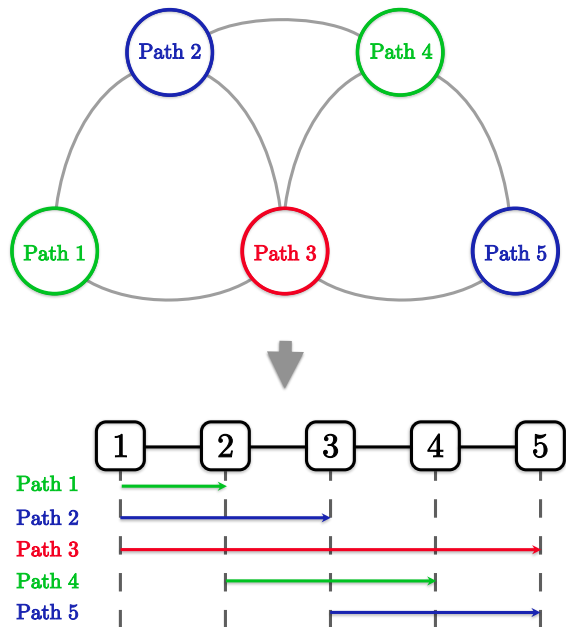


FIG. 2. An example of a graph coloring problem and its representation to the network graph with requests.

receiver. A single optical link can be shared between several paths given that each path is assigned different wavelengths. Each path is indicated by the path ID, which uniquely identifies a pair of transmitting/receiving nodes, sequence of interconnecting nodes, and the wavelength ID.

The WA problem implies allocation of the wavelength IDs for paths that are pre-computed and known *a priori* in such a way to meet the target objective, for example, the number of the used wavelengths is minimized¹. Formally, WA is considered to be correct if and only if it satisfies the following requirements: (i) each path should use a single wavelength and (ii) several paths sharing the same edge should have different wavelengths.

The problem of finding correct wavelength allocation under given constraints is equivalent to the coloring problem [7] in transformed graph $G = (V, E)$, where nodes V and edges E representing paths and their intersections in fibers, correspondingly (two nodes from V are connected if and only if the corresponding paths have an intersection within the optical network). Let N_V and N_E denote numbers of vertices and edges of G , respectively. Later we interchangeably use terms *wavelengths* and *colors* since the underlying problems are formally identical. The example of the correspondence of network paths to graph coloring mapping is shown in Fig. 2.

In order to define a particular coloring of graph G with at most W colors, we introduce a two collections of aux-

¹ We note that other objectives for optimization are also possible, such as total throughput or network resiliency.

iliary variables. The first variable is \mathbf{x} that consists of $N_V W$ binary variables

$$x_{vi} = \begin{cases} 1, & \text{if vertex } v \text{ is assigned wavelength } i, \\ 0, & \text{otherwise.} \end{cases} \quad (1)$$

The second one, denoted by \mathbf{w} , consists of W binary variables

$$w_i = \begin{cases} 1, & \text{if } i\text{-th wavelength is assigned,} \\ 0, & \text{otherwise.} \end{cases} \quad (2)$$

Employing \mathbf{x} and \mathbf{w} , the problem of finding an correct allocation with minimum number of the used wavelengths not exceeding some maximal number $W \geq 1$, can be formulated as an integer programming (IP) problem of the following form:

$$\sum_{i=1}^W w_i \rightarrow \min, \quad \text{s.t.} \quad (3)$$

$$\sum_{i=1}^W x_{vi} = 1 \quad \forall v \in V, \quad (4)$$

$$x_{ui} + x_{vi} \leq w_i \quad \forall i \in \{1, \dots, W\}, \forall (u, v) \in E. \quad (5)$$

One can see that constraint (4) assures that each vertex is assigned to exactly one wavelength, while constraint (5) indicates that two adjacent vertices are not assigned the same wavelength.

This problem is generally NP-hard, so its solution is computationally challenging for large sizes. As it is shown below, the QUBO reduction makes the problem compatible with quantum-inspired algorithms that can shift tractability boundaries to higher problem sizes. While such reduction usually involves additional overheads in the problem size due to auxiliary variables, the overheads can be compensated by the computational advantage of quantum-inspired solvers leading to better overall results.

III. RESULTS

A. Transforming the WA problem to a QUBO form

In order to make the WA problem compatible with the SimCIM quantum-inspired optimization algorithm [35], we first consider a transformation, allowing one to convert the IP problem (3)–(5) into a QUBO form as follows:

$$\mathbf{s}^T Q \mathbf{s} \rightarrow \min \quad (6)$$

for a certain binary vector \mathbf{s} and the symmetric real matrix Q . This problem is equivalent to finding a configuration of binary-state particles (“spins”) that minimizes the energy

$$\mathcal{H}(\mathbf{s}) = \mathbf{s}^T Q \mathbf{s}, \quad (7)$$

where the Ising Hamiltonian \mathcal{H} consists of only single-order terms (energies of individual spins in external magnetic field) and pair-wise interactions between spins. Although spin variables usually are considered to take values ± 1 , the transition to a binary form is quite straightforward [13].

A known way [7] to transform a graph coloring problem to the QUBO form, is to set $\mathbf{s} := \mathbf{x}$ (here we treat \mathbf{x} as a $N_V W$ -dimensional vector), and use the Hamiltonian of the form

$$\mathcal{H}(\mathbf{x}) = \mathcal{H}_1(\mathbf{x}) + \mathcal{H}_2(\mathbf{x}), \quad (8)$$

where

$$\mathcal{H}_1(\mathbf{x}) = \sum_{v=1}^{N_V} \left(1 - \sum_{i=1}^W x_{vi} \right)^2, \quad (9)$$

$$\mathcal{H}_2(\mathbf{x}) = \sum_{(u,v) \in E} \sum_{i=1}^W x_{ui} x_{vi}. \quad (10)$$

One can see that $\mathcal{H}_1(\mathbf{x}) > 0$ in the case where single node is assigned with two distinct colors, while $\mathcal{H}_2(\mathbf{x}) > 0$ when two adjacent vertices are assigned the same color. If minimization routine provides some \mathbf{x} such that $\mathcal{H}(\mathbf{x}) = 0$, then \mathbf{x} defines a correct coloring with at most W colors. Therefore, an ability to solve the QUBO problem corresponding to Hamiltonian (8) guarantees one to solve a decision problem of whether it is possible to color a graph with at most W colors. Since it is always possible to color a graph with $W = N_V$ colors, a minimal number of colors can be obtained, for example, by using a standard binary search with at most $\lceil \log_2(N_V) \rceil$ iterations. We note that this approach is quite sensitive to possible imperfections of QUBO problem solutions, especially at first iterations of the binary search. An alternative way is to decrease W by unit at each step, that however, results in a possible increase of iteration numbers up to $\mathcal{O}(W_{\text{start}})$, where W_{start} is the initial upper bound for colors number.

B. Improving QUBO transformation for quantum-inspired annealing

We propose an improved approach for solving graph coloring problem by developing an alternative transformation into a QUBO form. In our approach we pursue two major goals. The first is decreasing the number of QUBO problems to be solved. The second is making the whole algorithm robust against the possibility of finding not optimal, but some suboptimal solution for a particular QUBO problem. We note that these points are of particular importance in the framework of using (quantum-inspired) annealing for solving QUBO problems.

The main idea of our approach is to consider an extended $N_V(W+1)$ -dimensional binary vector $\mathbf{s} := (\mathbf{w}, \mathbf{x})$

and take the target Hamiltonian in the following form:

$$\mathcal{H}(\mathbf{w}, \mathbf{x}) = c_0 \mathcal{H}_0(\mathbf{w}) + c_1 [\mathcal{H}_1(\mathbf{x}) + \mathcal{H}_2(\mathbf{x})] + c_2 \mathcal{H}_3(\mathbf{w}, \mathbf{x}), \quad (11)$$

where

$$\mathcal{H}_0(\mathbf{w}) = \sum_{i=1}^W w_i, \quad (12)$$

$$\mathcal{H}_3(\mathbf{w}, \mathbf{x}) = \sum_{(u,v) \in E} \sum_{i=1}^W (1 - w_i) (x_{ui} + x_{vi}), \quad (13)$$

and c_i are positive coefficients satisfying a particular constraint (see more details in Methods [VA](#)). Minimization of this Hamiltonian provides us the solution vector (\mathbf{w}, \mathbf{x}) such that the optimal number of wavelength is encoded in \mathbf{w} by non-zero values. We note that the term $\mathcal{H}_0(\mathbf{w})$ grows with the total number of used wavelengths; $\mathcal{H}_1(\mathbf{x})$ and $\mathcal{H}_2(\mathbf{x})$ have the same form as in Eq. (8); and $\mathcal{H}_3(\mathbf{w}, \mathbf{x})$ is responsible for the relationship $w_i \geq x_{vi}$, which becomes positive when the relation is violated. Both terms $\mathcal{H}_2(\mathbf{x})$ and $\mathcal{H}_3(\mathbf{w}, \mathbf{x})$ correspond to inequalities (5) in the IP form (see Methods [V](#)).

The complete algorithm of solving graph coloring problem (WA problem) is shown in Algorithm 1. The algorithm employs a subroutine `make_qubo(G, W)` that generates the corresponding QUBO matrix Q with respect to Hamiltonian (11), given input graph G and the target number of the wavelengths W . The QUBO problem is then solved with subroutine `solve_qubo(Q)`, which finds the optimal spins vector $\mathbf{s} = (\mathbf{w}, \mathbf{x})$ using the quantum-inspired SimCIM approach for the QUBO matrix Q as defined in Ref. [35]. In order check the validness of obtained solution, we use `check_coloring(G, \mathbf{x})` that validates the fulfilment of Eq. (4) and Eq. (5).

Algorithm 1 Solving graph coloring problem with improved transformation

Require: W is the initial upper bound on the number of wavelengths

Require: `make_qubo(G, W)` $\rightarrow Q$

Require: `solve_qubo(Q)` $\rightarrow (\mathbf{w}, \mathbf{x})$

Require: `check_coloring(G, \mathbf{x})` \rightarrow true/false

returns true if coloring is correct

```

1:  $\mathbf{x}^{\text{opt}} := \mathbf{0}$  ▷ initializing solution variable
2:  $W' := W$  ▷ current number of colors
3: while  $W' \geq 1$  do
4:    $Q := \text{make\_qubo}(G, W')$ 
5:    $(\mathbf{w}, \mathbf{x}) := \text{solve\_qubo}(Q)$ 
6:   if check_coloring( $G, \mathbf{x}$ ) = true then
7:      $W' := \sum_{i=1}^{W'} w_i - 1$ 
8:      $\mathbf{x}^{\text{opt}} := \mathbf{x}$ 
9:   else
10:    break
11: return  $\mathbf{x}^{\text{opt}}$ 

```

One can see that, if `solve_qubo(Q)` provides an optimal solution, then the whole problem is solved in the first

iteration. However, even in the case when the obtained solution is sub-optimal, the updated problem with the reduced upper bound W becomes easier to solve, and the algorithm converges with a few numbers of iterations.

C. Numerical results

Here we solve the WA problem and obtain results with use of (i) the proposed technique based on quantum-inspired optimization SimCIM [35] (with the improved approach, see Methods), (ii) industry grade commercial Gurobi optimization software, and (iii) open-source mixed integer programming solver — GLPK. We note that in the case of the quantum-inspired optimization with SimCIM, we solve the problem in the QUBO form (11), whereas in case of Gurobi and GLPK we use the IP formulation of graph coloring [see Eqs. (3)–(5)]. Additionally, we include the results obtained via largest degree first (LDF) heuristics used as the baseline, since it allows one to instantly produce feasible coloring without numerical optimization. We also ran the experiments for original QUBO transformation proposed in Ref. [7] and compared them to our proposed QUBO in the Table [IV](#) in Appendix.

Number of nodes	LDF	GLPK	Gurobi	SimCIM
10	4.46	4.34	4.34	4.34
20	6.82	6.36	6.36	6.36
30	9.03	8.03	8.02	8.02
40	10.92	-	9.38	9.39
50	12.80	-	10.88	10.96
60	14.83	-	12.28	12.44
70	16.62	-	13.70	14.01
80	18.41	-	15.34	15.56
90	20.10	-	17.21	17.02
100	22.01	-	19.64	18.54

Average number of colors
(lower is better)

TABLE I. Numerical results obtained with largest degree first (LDF) heuristics, open-source mixed integer programming solver (GLPK), Gurobi optimization software, and SimCIM quantum-inspired optimization on number of colors averaged by number of nodes. The best result is highlighted in bold.

Our numerical experiments have been performed on a synthetic dataset of 900 randomly generated graphs with varying nodes number and edge probability (for details, see Methods [VC](#)). The main characteristics that we are interested in are time-to-solution (TTS) and the number of colors in the obtained solution. The total runtime has been limited by 300 seconds, and the the best solutions have been compared. Results are averaged over 90 runs for each graph size (for details, see Table [V](#)). For all numerical experiments, we use the same hardware set, which is based on Xeon E-2288G 3.7GHz CPU, 128GB RAM, and GeForce GTX1080 8GB graphics card.

Number of nodes	GLPK	Gurobi	SimCIM
10	1.77	0.002	0.19
20	103.97	0.02	0.45
30	195.39	0.12	4.95
40	-	0.79	8.90
50	-	14.63	16.82
60	-	38.89	28.51*
70	-	66.01	61.58*
80	-	102.14	69.00*
90	-	144.23	79.87
100	-	127.33	123.13

Average time (seconds)
(lower is better)

TABLE II. Mean solution time depending on the number of nodes for GLPK, Gurobi and SimCIM. The best result is highlighted in bold.

* cases, where average number of colors is higher

Our results indicate that the quantum-inspired technique SimCIM demonstrates behaviour comparable with Gurobi in the case of small (10-30 nodes). Moreover, the runtime of SimCIM is better for large-scale (90 and 100 nodes) graphs as it is indicated in Table II. Such trend can be explained. As the number of nodes increases, the number of inequalities in the ILP formulation of the problem grows rapidly. The number of inequalities is equal to the product of the number of edges by the number of colors available for coloring the vertices of the graph. So the complexity of the problem for the ILP solver increases rapidly with the number of nodes. GLPK shows a stable result up to 30 nodes and becomes unstable further after a timeout interrupt without any solution with more than 10 percent instances. We note that the comparison between our quantum-inspired approach and Gurobi is conducted in the common setting, so its additional tuning for obtaining better results is also possible. At the same time, we find it interesting that quantum-inspired technique shows comparable or superior results in harder, industry relevant combinatorial optimization problem.

D. Other potential applications

While our goal was to demonstrate the applicability of quantum-inspired graph coloring algorithm for wavelength assignment problem, our approach can be applied to a variety of problems, in particular from the field of scheduling [42].

Assuming we have the set of jobs to schedule, every job requires one time slot and some jobs can not be executed at the same time due to some interference with each other, we need to determine the minimal time when every job will be finished or how many time slots they will occupy. One can build the graph, so that vertices correspond to the jobs and two vertices are connected if these jobs can't be executed at the same time. The colors

of vertices represent time slots to assign, so graph has k number of colors if the jobs can be executed in k time slots.

Using our approach we take proposed Hamiltonian in Eq. (11) and redefine its variables so that

$$x_{vi} = \begin{cases} 1, & \text{if vertex } v \text{ is assigned time slot } i, \\ 0, & \text{otherwise,} \end{cases} \quad (14)$$

and

$$w_i = \begin{cases} 1, & \text{if } i\text{-th time slot is assigned,} \\ 0, & \text{otherwise.} \end{cases} \quad (15)$$

That way the jobs scheduling problem can be solved using quantum-inspired annealing analogously to WA problem.

The same approach can be implemented for tasks from other fields, such as computer register allocation [43], storage of chemicals [44] and printed circuit board testing [45].

IV. CONCLUSION

A search for new approaches to solving practically-relevant optimization problems is a clear goal for many industrial applications since even minor improvement on a large scale may generate serious economical impact. In this domain, much attention is paid to quantum computing, which is believed to be useful for such class of problems. At the current technological level, practical quantum advantage, for example, in optimization is still needed to be achieved. An interesting part of this research is understanding of the physical origin of the potential advantages of quantum computing technologies. Attempts to simulate quantum computation classically resulted in a new class of algorithms and methods known as quantum-inspired, which are ready to be tested for industry-relevant problems.

In this work, we have considered the industry important problem in the field of telecommunications. We have demonstrated a way to make it compatible with quantum and quantum-inspired techniques. Interestingly, our numerical results have indicated on an advantage of the quantum-inspired solver in a number of test cases against the industrial combinatorial solver working on the standard settings.

One may expect that the additional tuning of the industry grade commercial optimization solver may result in a substantial improving of its performance. At the same time, studying the origins of the advantages of the quantum-inspired approach, which are largely beyond the scope of the present proof-of-concept demonstration, would allow its further progress as well.

We would like to note that our comparison is limited by the upper bound of 100 nodes, since it allows us to run all solvers in equivalent hardware setup using CPU mode

on single core. Further analysis of larger graphs requires running SimCIM solver on GPU card, which gives significant acceleration factor not directly available in conventional MIP algorithms, which are heavily dependent on graph processing routines. As for the multi-core CPU execution environment, some MIP solvers can benefit from such setup by running various optimization strategies and hyperparameters simultaneously. Such speed up quickly reaches saturation point at the level of 8 16 cores (with around 2x improvement in accordance with Gurobi experiments, see slide 26 [46]) and demonstrates no substantial improvement at higher concurrency levels. On the other side, quantum-inspired approach exploits parallelism on the level of starting optimization points, which demonstrates slower, but stable performance increase at the higher levels of concurrency (100 ~ 1000 parallel units

of execution). Thus, we conduct our benchmarks exclusively using CPU mode on single-core to avoid bias towards either solution approach. In order to maintain fairness of comparison for larger graphs our benchmark routine should be further revised to account for heterogeneous (CPU/CPU multi-core vs GPU/multi-GPU) computing environments.

ACKNOWLEDGEMENTS

We acknowledge use of the Gurobi for this work; the views expressed are those of the authors and do not reflect the official policy or position of Gurobi. The part of this work related to the analysis of quantum-inspired optimization algorithm was supported by Russian Science Foundation (19-71-10092).

-
- [1] Paschos, V. T. (ed.) *Paradigms of combinatorial optimization*. ISTE. (John Wiley & Sons, Inc., London : Hoboken, 2014), 2nd ed. edn. URL <https://onlinelibrary.wiley.com/doi/book/10.1002/9781119005353>.
- [2] Farhi, E., Goldstone, J., Gutmann, S. & Sipser, M. Quantum computation by adiabatic evolution (2000). URL <https://arxiv.org/abs/quant-ph/0001106>.
- [3] Das, A. & Chakrabarti, B. K. Colloquium: Quantum annealing and analog quantum computation. *Rev. Mod. Phys.* **80**, 1061–1081 (2008). URL <https://link.aps.org/doi/10.1103/RevModPhys.80.1061>.
- [4] Albash, T. & Lidar, D. A. Adiabatic quantum computation. *Rev. Mod. Phys.* **90**, 015002 (2018). URL <https://link.aps.org/doi/10.1103/RevModPhys.90.015002>.
- [5] Fedorov, A. K., Gisin, N., Belousov, S. M. & Lvovsky, A. I. Quantum computing at the quantum advantage threshold: a down-to-business review (2022). URL <https://arxiv.org/abs/2203.17181>.
- [6] Farhi, E., Goldstone, J. & Gutmann, S. A quantum approximate optimization algorithm (2014). 1411.4028.
- [7] Lucas, A. Ising formulations of many NP problems. *Frontiers in Physics* **2**, 5 (2014).
- [8] King, A. D. *et al.* Scaling advantage over path-integral monte carlo in quantum simulation of geometrically frustrated magnets. *Nature Communications* **12**, 1113 (2021). URL <https://doi.org/10.1038/s41467-021-20901-5>.
- [9] Streif, M., Neukart, F. & Leib, M. Solving quantum chemistry problems with a d-wave quantum annealer. In Feld, S. & Linnhoff-Popien, C. (eds.) *Quantum Technology and Optimization Problems*, 111–122 (Springer International Publishing, Cham, 2019).
- [10] Chermoshentsev, D. A. *et al.* Polynomial unconstrained binary optimisation inspired by optical simulation (2021). 2106.13167.
- [11] Perdomo-Ortiz, A., Dickson, N., Drew-Brook, M., Rose, G. & Aspuru-Guzik, A. Finding low-energy conformations of lattice protein models by quantum annealing. *Scientific Reports* **2**, 571 (2012). URL <https://doi.org/10.1038/srep00571>.
- [12] Babej, T., Ing, C. & Fingerhuth, M. Coarse-grained lattice protein folding on a quantum annealer (2018). 1811.00713.
- [13] Boev, A. S. *et al.* Genome assembly using quantum and quantum-inspired annealing. *Scientific Reports* **11**, 13183 (2021). URL <https://doi.org/10.1038/s41598-021-88321-5>.
- [14] Sarkar, A., Al-Ars, Z. & Bertels, K. Quaser: Quantum accelerated de novo dna sequence reconstruction. *PLOS ONE* **16**, 1–23 (2021). URL <https://doi.org/10.1371/journal.pone.0249850>.
- [15] Chang, C. C., Gambhir, A., Humble, T. S. & Sota, S. Quantum annealing for systems of polynomial equations. *Scientific Reports* **9**, 10258 (2019). URL <https://doi.org/10.1038/s41598-019-46729-0>.
- [16] Orús, R., Mugel, S. & Lizaso, E. Quantum computing for finance: Overview and prospects. *Reviews in Physics* **4**, 100028 (2019). URL <https://www.sciencedirect.com/science/article/pii/S2405428318300571>.
- [17] Mugel, S. *et al.* Dynamic portfolio optimization with real datasets using quantum processors and quantum-inspired tensor networks (2020). 2007.00017.
- [18] Grant, E., Humble, T. S. & Stump, B. Benchmarking quantum annealing controls with portfolio optimization. *Phys. Rev. Applied* **15**, 014012 (2021). URL <https://link.aps.org/doi/10.1103/PhysRevApplied.15.014012>.
- [19] Herman, D. *et al.* A survey of quantum computing for finance (2022). URL <https://arxiv.org/abs/2201.02773>.
- [20] Orús, R., Mugel, S. & Lizaso, E. Forecasting financial crashes with quantum computing. *Phys. Rev. A* **99**, 060301 (2019). URL <https://link.aps.org/doi/10.1103/PhysRevA.99.060301>.
- [21] Rosenberg, G. *et al.* Solving the optimal trading trajectory problem using a quantum annealer. *IEEE Journal of Selected Topics in Signal Processing* **10**, 1053–1060 (2016).
- [22] Rosenberg, G. Finding optimal arbitrage opportunities using a quantum annealer (2016). URL <https://1qbit.com/>.

- [23] Andrew Milne, M. R. & Goddard, P. Optimal feature selection in credit scoring and classification using a quantum annealer (2017). URL <https://1qbit.com/>.
- [24] Vesely, M. Application of quantum computers in foreign exchange reserves management (2022). URL <https://arxiv.org/abs/2203.15716>.
- [25] Neukart, F. *et al.* Traffic flow optimization using a quantum annealer. *Frontiers in ICT* **4**, 29 (2017). URL <https://www.frontiersin.org/article/10.3389/fict.2017.00029>.
- [26] Inoue, D., Okada, A., Matsumori, T., Aihara, K. & Yoshida, H. Traffic signal optimization on a square lattice with quantum annealing. *Scientific Reports* **11**, 3303 (2021). URL <https://doi.org/10.1038/s41598-021-82740-0>.
- [27] Hussain, H., Javaid, M. B., Khan, F. S., Dalal, A. & Khalique, A. Optimal control of traffic signals using quantum annealing. *Quantum Information Processing* **19**, 312 (2020). URL <https://doi.org/10.1007/s11128-020-02815-1>.
- [28] Venturelli, D., Marchand, D. J. J. & Rojo, G. Quantum annealing implementation of job-shop scheduling (2016). 1506.08479.
- [29] Ikeda, K., Nakamura, Y. & Humble, T. S. Application of quantum annealing to nurse scheduling problem. *Scientific Reports* **9**, 12837 (2019). URL <https://doi.org/10.1038/s41598-019-49172-3>.
- [30] Sadhu, A., Zaman, S., Das, K., Banerjee, A. & Khan, F. Quantum annealing for solving a nurse-physician scheduling problem in covid-19 clinics (2020).
- [31] Stollenwerk, T. *et al.* Image acquisition planning for earth observation satellites with a quantum annealer (2020). 2006.09724.
- [32] Domino, K., Koniorczyk, M., Krawiec, K., Jałowicki, K. & Gardas, B. Quantum computing approach to railway dispatching and conflict management optimization on single-track railway lines (2021). 2010.08227.
- [33] Domino, K. *et al.* Quantum annealing in the nisq era: railway conflict management (2021). 2112.03674.
- [34] Ebadi, S. *et al.* Quantum optimization of maximum independent set using rydberg atom arrays. *Science* **376**, 1209–1215 (2022). URL <https://www.science.org/doi/abs/10.1126/science.abo6587>. <https://www.science.org/doi/pdf/10.1126/science.abo6587>.
- [35] Tiunov, E. S., Ulanov, A. E. & Lvovsky, A. I. Annealing by simulating the coherent ising machine. *Opt. Express* **27**, 10288–10295 (2019). URL <http://opg.optica.org/oe/abstract.cfm?URI=oe-27-7-10288>.
- [36] Killoran, N. *et al.* Continuous-variable quantum neural networks. *Phys. Rev. Research* **1**, 033063 (2019). URL <https://link.aps.org/doi/10.1103/PhysRevResearch.1.033063>.
- [37] Oshiyama, H. & Ohzeki, M. Benchmark of quantum-inspired heuristic solvers for quadratic unconstrained binary optimization. *Scientific Reports* **12**, 2146 (2022). URL <https://doi.org/10.1038/s41598-022-06070-5>.
- [38] Resende, M. G. C. Combinatorial optimization in telecommunications. In *Applied Optimization*, 59–112 (Springer US, 2003). URL https://doi.org/10.1007/978-1-4613-0233-9_4.
- [39] Vesselinova, N., Steinert, R., Perez-Ramirez, D. F. & Boman, M. Learning combinatorial optimization on graphs: A survey with applications to networking. *IEEE Access* **8**, 120388–120416 (2020).
- [40] Martin, V. *et al.* Quantum technologies in the telecommunications industry. *EPJ Quantum Technology* **8**, 19 (2021). URL <https://doi.org/10.1140/epjqt/s40507-021-00108-9>.
- [41] Harwood, S. *et al.* Formulating and solving routing problems on quantum computers. *IEEE Transactions on Quantum Engineering* **2**, 1–17 (2021).
- [42] Marx, D. Graph colouring problems and their applications in scheduling. *Periodica Polytechnica Electrical Engineering (Archives)* **48**, 11–16 (2004).
- [43] Chaitin, G. J. *et al.* Register allocation via coloring. *Computer languages* **6**, 47–57 (1981).
- [44] Ott, J., Tan, D., Loveless, T., Grover, W. H. & Brisk, P. Chemstor: using formal methods to guarantee safe storage and disposal of chemicals. *Journal of chemical information and modeling* **60**, 3416–3422 (2020).
- [45] Garey, M., Johnson, D. & So, H. An application of graph coloring to printed circuit testing. *IEEE Transactions on circuits and systems* **23**, 591–599 (1976).
- [46] Glockner, G. Parallel and distributed optimization with gurobi optimizer. URL: <https://assets.gurobi.com/pdfs/2015-09-21-Parallel-and-Distributed-Optimization-with-the-Gurobi-Optimizer.pdf> (2015).
- [47] Batagelj, V. & Brandes, U. Efficient generation of large random networks. *Physical Review E* **71** (2005). Article Number: 36113.

V. METHODS

A. Hamiltonian of wavelength assignment problem

The main step in solving an optimization problem using quantum and quantum-inspired annealing is to map the problem of interest to the energy Hamiltonian (so-called Ising Hamiltonian), so the quantum device could find the ground state that corresponds to the optimum value of the objective function. Here we formulate a mapping of the graph coloring problem into QUBO form given by Eq. (6). There is a well-known transformation of the graph $G = (V, E)$ coloring decision model [7] that shows possibility of coloring with some constant number of colors W , but we represent novel QUBO transformation that could minimize number of colors and implement original problem statement Eq. (3-5).

The objective function $\sum_{i=1}^W w_i$ could be exactly mapped to the QUBO form:

$$\mathcal{H}_0(\mathbf{w}) = \sum_{i=1}^W w_i, \quad (16)$$

where, recall, $\mathbf{w} = (w_1, \dots, w_W)$ is a binary vector indicating colors used in coloring. The constraint $\sum_{i=1}^W x_{vi} = 1$ for every $v \in V$ after mapping takes the form

$$\mathcal{H}_1(\mathbf{x}) = \sum_{v=1}^{N_V} \left(1 - \sum_{i=1}^W x_{vi} \right)^2, \quad (17)$$

where N_V is the number of nodes in G .

The situation with the second constraint $x_{ui} + x_{vi} \leq w_i$ for every $i \in \{1, \dots, W\}$ and $(u, v) \in E$ appears to be more complicated. One can see that it involves three variables, and thus can not be directly embedded into a two-body Hamiltonian. However, we can use the following trick. One can easily check that for arbitrary $a, b, c \in \{0, 1\}$, the following equivalence holds:

$$a + b \leq c \Leftrightarrow \begin{cases} ab = 0, \\ (1 - c)(a + b) = 0. \end{cases} \quad (18)$$

This fact allows us to embed the conditions $x_{ui} + x_{vi} \leq w_i$ into two Hamiltonians:

$$\mathcal{H}_2(\mathbf{x}) = \sum_{(u,v) \in E} \sum_{i=1}^W x_{ui} x_{vi}, \quad (19)$$

$$\mathcal{H}_3(\mathbf{w}, \mathbf{x}) = \sum_{(u,v) \in E} \sum_{i=1}^W (1 - w_i) (x_{ui} + x_{vi}). \quad (20)$$

The resulting Hamiltonian consist of all components sum:

$$\mathcal{H}(\mathbf{w}, \mathbf{x}) = c_0 \mathcal{H}_0(\mathbf{w}) + c_1 [\mathcal{H}_1(\mathbf{x}) + \mathcal{H}_2(\mathbf{x})] + c_2 \mathcal{H}_3(\mathbf{w}, \mathbf{x}), \quad (21)$$

where c_0 , c_1 , and c_2 are positive constants stand for a positive penalty value. We note that the sum $\mathcal{H}_1(\mathbf{x}) + \mathcal{H}_2(\mathbf{x})$ is exactly matched with the classical decision problem [7] and responsible for the correct coloring of the graph. Therefore, $\mathcal{H}_1(\mathbf{x})$, $\mathcal{H}_2(\mathbf{x})$ are grouped with the same penalty coefficient c_1 . Coefficients c_0 , c_1 , and c_2 should be set manually, using the following criteria: the penalty value c_1 should be high enough to keep the final solution from violating constraints. At the same time, too big penalty value can overwhelm the target function, making it difficult to distinguish solutions of different qualities. We establish inequalities for constraint coefficients that show the equivalence of IP and QUBO models of a problem.

Proposition (QUBO penalty coefficients selection). Consider an IP problem given by Eq. (3)-(5) for some maximal colors number W and some graph $G = (V, E)$ with N_E edges. If the IP problem has a solution, then the corresponding QUBO problem, given by Hamiltonian (21) with penalty coefficients satisfying

$$c_1 > 2N_E W c_2 + W c_0, \quad (22)$$

$$c_2 > W c_0, \quad (23)$$

has a solution, equivalent to the solution of the IP problem.

Proof. First, let us rewrite Hamiltonian (21) in the form

$$\mathcal{H}(\mathbf{w}, \mathbf{x}) = c_0 \mathcal{A}(\mathbf{w}) + c_1 \mathcal{B}(\mathbf{x}) + c_2 \mathcal{C}(\mathbf{w}, \mathbf{x}), \quad (24)$$

where

$$\begin{aligned} \mathcal{A}(\mathbf{w}) &:= \mathcal{H}_0(\mathbf{w}), \\ \mathcal{B}(\mathbf{x}) &:= \mathcal{H}_1(\mathbf{x}) + \mathcal{H}_2(\mathbf{x}), \\ \mathcal{C}(\mathbf{w}, \mathbf{x}) &:= \mathcal{H}_3(\mathbf{w}, \mathbf{x}). \end{aligned} \quad (25)$$

Note that \mathcal{A} , \mathcal{B} , and \mathcal{C} can take non negative integer values only. Let $(\mathbf{w}_I, \mathbf{x}_I)$ and $(\mathbf{w}_Q, \mathbf{x}_Q)$ be solutions of the IP and QUBO problems correspondingly. Our goal is to prove that (i)

$$\mathcal{B}(\mathbf{x}_Q) = \mathcal{C}(\mathbf{w}_Q, \mathbf{x}_Q) = 0, \quad (26)$$

i.e., $(\mathbf{x}_Q, \mathbf{w}_Q)$ defines a correct coloring, and (ii)

$$\mathcal{A}(\mathbf{w}_Q) = \sum_{i=1}^W (\mathbf{w}_I)_i, \quad (27)$$

i.e., the solution of the QUBO problem coincides with the one of the IP problem.

First, let us see that Eq. (22) assures $\mathcal{B}(\mathbf{x}_Q) = 0$. The proof of this part is by a contradiction. Suppose that $\mathcal{B}(\mathbf{x}_Q) \geq 1$. Consider the difference of energy functions

$$\begin{aligned} \Delta \mathcal{H} &:= \mathcal{H}(\mathbf{w}_Q, \mathbf{x}_Q) - \mathcal{H}(\mathbf{w}_I, \mathbf{x}_I) \\ &= c_0 [\mathcal{A}(\mathbf{w}_Q) - \mathcal{A}(\mathbf{w}_I)] + c_1 [\mathcal{B}(\mathbf{x}_Q) - \mathcal{B}(\mathbf{x}_I)] \\ &\quad + c_2 [\mathcal{C}(\mathbf{w}_Q, \mathbf{x}_Q) - \mathcal{C}(\mathbf{w}_I, \mathbf{x}_I)]. \end{aligned} \quad (28)$$

The correctness of the IP solution implies $\mathcal{B}(\mathbf{x}_I) = 0$, and so $\mathcal{B}(\mathbf{x}_Q) - \mathcal{B}(\mathbf{x}_I) \geq 1$. The differences in terms with \mathcal{A} and \mathcal{C} can be lower bounded by the corresponding extreme values:

$$\mathcal{A}(\mathbf{w}_Q) - \mathcal{A}(\mathbf{w}_I) \geq -W, \quad (29)$$

$$\mathcal{C}(\mathbf{w}_Q, \mathbf{x}_Q) - \mathcal{C}(\mathbf{w}_I, \mathbf{x}_I) \geq -2N_E W. \quad (30)$$

In this way, Eq. (28) transforms into

$$\Delta \mathcal{H} \geq -c_0 W + c_1 - 2c_2 N_E W > 0, \quad (31)$$

given constraint (22). However, this result contradicts with the fact that $(\mathbf{w}_Q, \mathbf{x}_Q)$ provides the minimal energy. Therefore, $\mathcal{B}(\mathbf{x}_Q) = 0$, and

$$\mathcal{H}(\mathbf{w}_Q, \mathbf{x}_Q) = c_0 \mathcal{A}(\mathbf{w}_Q) + c_2 \mathcal{C}(\mathbf{w}_Q, \mathbf{x}_Q). \quad (32)$$

We then prove that $\mathcal{C}(\mathbf{w}_Q, \mathbf{x}_Q)$ is zero as well. Indeed, if $\mathcal{C}(\mathbf{w}_Q, \mathbf{x}_Q) \geq 1$, then

$$\begin{aligned} \Delta \mathcal{H} &= c_0 [\mathcal{A}(\mathbf{w}_Q) - \mathcal{A}(\mathbf{w}_I)] \\ &\quad + c_2 [\mathcal{C}(\mathbf{w}_Q, \mathbf{x}_Q) - \mathcal{C}(\mathbf{w}_I, \mathbf{x}_I)] \\ &\geq -c_0 W + c_2 > 0, \end{aligned} \quad (33)$$

provided $\mathcal{C}(\mathbf{w}_I, \mathbf{x}_I) = 0$ and the second constraint (23). Thus, $\mathcal{H}(\mathbf{w}_Q, \mathbf{x}_Q) = c_0 \mathcal{A}(\mathbf{w}_Q)$.

Finally, $\mathcal{A}(\mathbf{w}_Q) = \mathcal{A}(\mathbf{w}_I)$, since otherwise, either there exist a solution for the QUBO problem that is better than $(\mathbf{w}_Q, \mathbf{x}_Q)$, or $(\mathbf{x}_I, \mathbf{w}_I)$ is not the true solution the IP problem.

Therefore, the optimal solution to the QUBO problem appears to be equivalent to the optimal solution to the corresponding IP problem.

B. Wavelength assignment QUBO transformation

Here we demonstrate how to construct an operator matrix Q of our QUBO model for the WA problem. Recall that we take the binary vector of the QUBO problem in the form $\mathbf{s} = (\mathbf{w}, \mathbf{x})$, i.e. enumerate $K = (N_V + 1)W$ binary variables s_k and link them to our model variables as follows:

$$s_k = \begin{cases} w_k, & k = 1, \dots, W, \\ x_{ui}, & k = uW + i, \end{cases} \quad (34)$$

where $u = 1, \dots, N_V, i = 1, \dots, W$.

The goal is to find vector \mathbf{s} that minimizes quadratic form $\mathbf{s}^T Q \mathbf{s}$ and we show that it is equivalent to minimizing energy of Hamiltonian (11). Let us denote A the adjacency matrix of network graph $G = (V, E)$ so that $a_{uv} = 1$ if $(u, v) \in E$ and $a_{uv} = 0$ otherwise. We note that sum of v -th column of A equals the degree of the vertex v and the sum of all vertex degrees is $2N_E$. We rewrite operator (11) terms $\mathcal{H}_0(\mathbf{w})$, $\mathcal{H}_1(\mathbf{x})$, $\mathcal{H}_2(\mathbf{x})$ and $\mathcal{H}_3(\mathbf{w}, \mathbf{x})$ as follows:

$$\mathcal{H}_0(\mathbf{w}) = \sum_{i=1}^W w_i^2, \quad (35)$$

$$\begin{aligned} \mathcal{H}_1(\mathbf{x}) &= \sum_{v=1}^{N_V} \left(1 - \sum_{i=1}^W x_{vi} \right)^2 = \\ &= \sum_{v=1}^{N_V} \left(\left(\sum_{i=1}^W x_{vi} \right)^2 - 2 \sum_{i=1}^W x_{vi} \right) + N_V = \\ &= \sum_{v=1}^{N_V} \left(\sum_{i,j=1}^W x_{vi} x_{vj} - 2 \sum_{i=1}^W x_{vi}^2 \right) + N_V, \end{aligned} \quad (36)$$

$$\mathcal{H}_2(\mathbf{x}) = \sum_{(u,v) \in E} \sum_{i=1}^W x_{ui} x_{vi} = \sum_{u,v=1}^{N_V} \sum_{i=1}^W a_{uv} x_{ui} x_{vi}, \quad (37)$$

$$\begin{aligned} \mathcal{H}_3(\mathbf{w}, \mathbf{x}) &= \sum_{(u,v) \in E} \sum_{i=1}^W (1 - w_i) (x_{ui} + x_{vi}) = \\ &= \sum_{i=1}^W (1 - w_i) \sum_{v=1}^{N_V} d_v x_{vi} = \\ &= \sum_{v=1}^{N_V} \sum_{i=1}^W d_v w_i x_{vi} + \sum_{v=1}^{N_V} d_v \sum_{i=1}^W x_{vi}. \end{aligned} \quad (38)$$

In expanding the expression for $\mathcal{H}_1(\mathbf{x})$ we exploit the fact that since x_{vi} is binary then $x_{vi}^2 = x_{vi}$. Also we note that if $\mathcal{H}_1(\mathbf{x}) = 0$ then the last term in $\mathcal{H}_3(\mathbf{w}, \mathbf{x})$ equals $2N_E$.

Considering the equalities (35-38) for Hamiltonian terms $\mathcal{H}_0(\mathbf{x})$, $\mathcal{H}_1(\mathbf{x})$, $\mathcal{H}_2(\mathbf{x})$ and $\mathcal{H}_3(\mathbf{w}, \mathbf{x})$, we construct QUBO operator as block matrix as follows:

$$Q = \begin{pmatrix} Q_{11} & Q_{12} \\ Q_{21} & Q_{22} \end{pmatrix}, \quad (39)$$

where

$$Q_{11} = c_0 E_W, \quad (40)$$

$$Q_{12} = -\frac{c_2}{2} D \otimes E_W, \quad Q_{21} = Q_{12}^T, \quad (41)$$

$$Q_{22} = c_1 E_{N_V} \otimes (I_W - 2E_W) + c_1 A \otimes E_W. \quad (42)$$

Here E_W denotes the identity matrix of size W , I_W denotes a matrix with all elements equal to 1 of those of size W , and $D = (d_1, \dots, d_{N_V})$ is a row vector of graph vertex degrees. We also employ the fact that terms of the form

$$\sum_{u,v=1}^{N_V} \sum_{i,j=1}^W c_{uv} h_{ij} x_{ui} x_{vj}, \quad (43)$$

for some coefficients $c_{uv} = c_{vu}$ and $h_{ij} = h_{ji}$ can be represented by a quadratic form defined by Kronecker product $C \otimes H$, where C and H are matrices of c_{uv} and h_{ij} correspondingly. One can that matrix Q is constructed so that Q_{11} submatrix corresponds to the term $\mathcal{H}_0(\mathbf{x})$ of Hamiltonian (11), Q_{12} submatrix is for $\mathcal{H}_3(\mathbf{w}, \mathbf{x})$ and Q_{22} is for $\mathcal{H}_1(\mathbf{x}) + \mathcal{H}_2(\mathbf{x})$.

It is worth to emphasize that it is the structure of encoding problem parameters into the spin vector, given by (34), that allow us to represent submatrices Q_{12} , Q_{21} , and Q_{22} in the form of Kronecker products. This feature of QUBO submatrices significantly speeds up their assembly using standard mathematical packages, e.g., numpy and scipy.

C. Dataset generation

We generate dataset are used binomial graphs [47], or Erdős-Rényi graphs, which have two parameters for generation: the number of nodes N_V and the probability of an edge occurrence p . Each of possible $N = N_V \cdot (N_V - 1) / 2$ edges is chosen with probability p . Number of edges N_E are drawn randomly from binomial distribution:

$$P(N_E = x) = \binom{N}{x} p^x \cdot q^{(N-x)}. \quad (44)$$

To take into account sparse and dense graphs, various probability p options from 0.1 to 0.9 with an interval of 0.1 have been chosen, the number of graph nodes has been varied from 10 to 100 with a step of 10. For each pair (n, p) , 10 connected graphs have been generated with different seed parameters. We note that disconnected graphs are not included the dataset. The overall characteristics of the dataset are given in the Table III.

Number of nodes	Number of edges		QUBO matrix size	
	min	max	min	max
10	9	43	44	110
20	23	176	84	315
30	39	399	124	589
40	74	714	205	943
50	118	1123	255	1377
60	168	1625	366	1891
70	231	2209	426	2556
80	301	2879	486	3321
90	372	3652	546	4004
100	470	4501	707	4848

TABLE III. Characteristics of graph coloring dataset, the total number of instances is 900.

D. Setting penalty values

Optimal penalty values guarantee the fulfilment of constraints for an optimal solution, but large values of c_1 and c_2 reduce the contribution of the initial objective function to the total energy and significantly increase the time to find the optimal solution. Our approach to solve this problem is as follows:

1. Set the minimum possible penalty values c_1 and c_2 using trial runs, so that the contribution of the objective function is sufficient;
2. Use all SimCIM iterations to select feasible solutions;
3. Take the feasible solution with the lowest energy.

The following penalty values were set for the tests:

$$c_0 = 1, c_1 = 10 + pN_V, c_2 = 2.5. \quad (45)$$

E. Quantum-inspired annealing using SimCIM

SimCIM [35] is an example of a quantum-inspired annealing algorithm, which works in an iterative manner. SimCIM can be used for sampling low-energy spin configurations in the classical Ising model which Hamiltonian can be written as:

$$\mathcal{H} = \sum_i h_i s_i + \sum_{\langle i,j \rangle} J_{ij} s_i s_j, \quad (46)$$

where J represents the spin-spin interaction, h represents the external field, and the s_i are the individual spins on each of the lattice sites. The Ising Hamiltonian can be directly transformed to a QUBO problem [13] and then quantum annealing can be applied to any optimization problem, which can be expressed into the QUBO form.

The SimCIM algorithm treats each spin value as a continuous variable $s_i \in [-1, 1]$. Each iteration of the algorithm starts with calculating the mean field of the following form:

$$\Phi_i = \sum_{j \neq i} J_{ij} s_j + h_i, \quad (47)$$

which act on each spin by all other spins. Then the gradients for the spin values are calculated as follows:

$$\Delta s_i = p_t s_i + \zeta \Phi_i + N(0, \sigma), \quad (48)$$

where p_t is a dynamic parameter dependent on SimCIM annealing process, overall feedforward factor ζ and $N(0, \sigma)$ is a random variable sampled from the Gaussian distribution with zero mean and standard deviation σ .

Then the spin values are updated according to $s_i \leftarrow \phi(s_i + \Delta s_i)$, where $\phi(x)$ is the activation function

$$\phi(x) = \begin{cases} x & \text{for } |x| \leq 1; \\ x/|x|, & \text{otherwise.} \end{cases} \quad (49)$$

After multiple updates, the spins will tend to either -1 or $+1$ and the final discrete spin configuration is obtained by taking the sign of each s_i .

In our implementation we add several improvements to SimCIM algorithm defined in the original paper [35]. In particular, we normalize the value of the Gaussian noise to gradient norm and introduced gradient quantization, which made the solver more stable near optimum points.

APPENDIX

Number of nodes	Original QUBO transformation		Proposed QUBO transformation	
	Number of colors	Run time	Number of colors	Run time
10	4.34	0.28	4.34	0.19
20	6.47	0.62	6.36	0.45
30	8.24	7.67	8.02	4.95
40	10.31	14.22	9.39	8.90
50	12.41	26.28	10.96	16.82
60	14.53	42.01	12.44	28.51
70	16.52	63.89	14.01	61.58
80	18.03	98.50	15.56	69.00
90	19.74	106.61	17.02	79.87
100	20.65	140.41	18.54	123.13

Average results
(lower is better)

TABLE IV. Comparison of proposed QUBO transformation for graph coloring problem to Original QUBO transformation described in Ref. [7]. Experiments were performed on the same dataset of 900 randomly generated graphs with the use of SimCIM. Results shows that the proposed QUBO runs faster, giving on average lower or the same number of colors.

SUPPLEMENTARY MATERIAL

Number of colors

TABLE V: Numerical results obtained with largest degree first (LDF) heuristics, open-source mixed integer programming solver (GLPK), Gurobi optimization software, and SimCIM quantum-inspired optimization on number of colors averaged by 10 graph with different number of nodes (N_V) and edge probability (p). The best result is highlighted in bold. SimCIM shows the best results in the p range $[0.3, \dots, 0.7]$.

	N_V	p	LDF		GLPK		Gurobi		SimCIM	
			mean	std	mean	std	mean	std	mean	std
1	10	0.1	3.0	0.000	2.50	0.527	2.5	0.527	2.5	0.527
2	10	0.2	3.0	0.000	3.00	0.000	3.0	0.000	3.0	0.000
3	10	0.3	3.1	0.316	3.10	0.316	3.1	0.316	3.1	0.316
4	10	0.4	3.6	0.516	3.50	0.527	3.5	0.527	3.5	0.527
5	10	0.5	4.0	0.471	4.00	0.471	4.0	0.471	4.0	0.471
6	10	0.6	4.7	0.675	4.50	0.527	4.5	0.527	4.5	0.527
7	10	0.7	5.2	0.422	5.00	0.667	5.0	0.667	5.0	0.667
8	10	0.8	5.9	0.994	5.90	0.994	5.9	0.994	5.9	0.994
9	10	0.9	7.6	0.843	7.60	0.843	7.6	0.843	7.6	0.843
10	20	0.1	3.0	0.000	3.00	0.000	3.0	0.000	3.0	0.000
11	20	0.2	3.7	0.675	3.50	0.527	3.5	0.527	3.5	0.527
12	20	0.3	4.4	0.516	4.10	0.316	4.1	0.316	4.1	0.316
13	20	0.4	5.6	0.516	5.00	0.000	5.0	0.000	5.0	0.000
14	20	0.5	6.3	0.949	5.70	0.483	5.7	0.483	5.7	0.483
15	20	0.6	7.5	0.527	6.80	0.422	6.8	0.422	6.8	0.422
16	20	0.7	8.4	0.843	7.40	0.516	7.4	0.516	7.4	0.516
17	20	0.8	10.0	0.816	9.20	0.632	9.2	0.632	9.2	0.632
18	20	0.9	12.5	0.850	12.50	0.850	12.5	0.850	12.5	0.850
19	30	0.1	3.6	0.516	3.00	0.000	3.0	0.000	3.0	0.000
20	30	0.2	4.7	0.483	4.00	0.000	4.0	0.000	4.0	0.000
21	30	0.3	6.0	0.000	5.00	0.000	5.0	0.000	5.0	0.000
22	30	0.4	7.2	0.422	6.00	0.000	6.0	0.000	6.0	0.000
23	30	0.5	8.3	0.675	7.20	0.422	7.2	0.422	7.2	0.422
24	30	0.6	9.8	0.919	8.60	0.516	8.5	0.527	8.5	0.527
25	30	0.7	11.5	0.850	10.50	0.972	10.1	0.738	10.1	0.738
26	30	0.8	13.7	0.949	13.40	0.966	12.6	0.699	12.6	0.699
27	30	0.9	16.5	1.509	16.25	1.669	15.8	1.398	15.8	1.398
28	40	0.1	4.0	0.000	-	-	3.1	0.316	3.1	0.316
29	40	0.2	5.3	0.483	-	-	4.5	0.527	4.5	0.527
30	40	0.3	7.1	0.568	-	-	6.0	0.000	6.0	0.000
31	40	0.4	8.5	0.527	-	-	6.9	0.316	6.9	0.316
32	40	0.5	10.1	0.738	-	-	8.3	0.483	8.4	0.516
33	40	0.6	12.3	0.823	-	-	9.9	0.316	9.9	0.316
34	40	0.7	13.8	0.919	-	-	11.8	0.632	11.8	0.632
35	40	0.8	16.9	0.738	-	-	14.9	0.738	15.0	0.816
36	40	0.9	20.3	1.160	-	-	19.0	0.943	19.0	0.943
37	50	0.1	4.4	0.516	-	-	4.0	0.000	4.0	0.000
38	50	0.2	6.2	0.422	-	-	5.0	0.000	5.0	0.000
39	50	0.3	7.8	0.422	-	-	6.5	0.527	6.7	0.483
40	50	0.4	10.2	0.422	-	-	7.9	0.316	7.9	0.316
41	50	0.5	11.9	0.568	-	-	9.8	0.422	9.7	0.483
42	50	0.6	14.1	0.568	-	-	11.3	0.483	11.5	0.527
43	50	0.7	16.2	0.789	-	-	13.8	0.632	14.2	0.632
44	50	0.8	20.2	0.632	-	-	17.1	0.568	17.2	0.422
45	50	0.9	24.2	1.229	-	-	22.5	1.179	22.5	1.179
46	60	0.1	5.3	0.483	-	-	4.0	0.000	4.0	0.000
47	60	0.2	7.3	0.483	-	-	5.7	0.483	5.8	0.422
48	60	0.3	8.7	0.675	-	-	7.0	0.000	7.0	0.000

49	60	0.4	11.4	0.699	-	-	9.0	0.000	9.0	0.000
50	60	0.5	13.8	0.632	-	-	10.9	0.316	10.9	0.316
51	60	0.6	16.3	1.160	-	-	12.9	0.316	12.9	0.316
52	60	0.7	18.8	1.135	-	-	15.8	0.422	16.1	0.568
53	60	0.8	23.2	0.789	-	-	19.4	0.516	19.9	0.568
54	60	0.9	28.7	1.059	-	-	25.8	0.789	26.0	0.816
55	70	0.1	5.4	0.516	-	-	4.0	0.000	4.0	0.000
56	70	0.2	7.7	0.675	-	-	6.0	0.000	6.0	0.000
57	70	0.3	9.7	0.675	-	-	8.0	0.000	7.9	0.316
58	70	0.4	12.3	0.675	-	-	10.1	0.316	10.5	1.269
59	70	0.5	15.2	0.632	-	-	12.3	0.483	12.5	0.527
60	70	0.6	18.4	0.516	-	-	14.9	0.316	14.6	0.699
61	70	0.7	22.0	1.247	-	-	17.8	0.422	17.9	0.316
62	70	0.8	26.4	1.713	-	-	21.6	0.699	22.1	0.568
63	70	0.9	32.5	1.269	-	-	28.6	0.966	29.2	0.789
64	80	0.1	5.7	0.483	-	-	4.3	0.483	4.8	0.422
65	80	0.2	8.3	0.483	-	-	6.4	0.516	6.8	0.422
66	80	0.3	11.2	0.632	-	-	8.9	0.316	8.9	0.316
67	80	0.4	13.5	0.527	-	-	11.6	0.516	11.0	0.000
68	80	0.5	16.9	0.994	-	-	14.2	0.632	13.6	0.516
69	80	0.6	20.5	0.972	-	-	16.6	0.516	16.9	1.853
70	80	0.7	23.5	0.972	-	-	20.0	0.667	20.2	0.632
71	80	0.8	29.5	1.650	-	-	24.6	0.699	24.9	0.738
72	80	0.9	36.6	2.119	-	-	31.5	1.179	32.5	1.354
73	90	0.1	5.9	0.316	-	-	4.9	0.316	5.0	0.000
74	90	0.2	9.2	0.632	-	-	7.0	0.000	7.0	0.000
75	90	0.3	12.2	0.632	-	-	9.7	0.483	9.5	0.527
76	90	0.4	15.2	0.632	-	-	12.9	0.316	12.0	0.471
77	90	0.5	18.3	0.949	-	-	15.6	0.699	15.1	0.568
78	90	0.6	22.2	0.919	-	-	19.8	0.789	18.3	0.483
79	90	0.7	26.0	1.333	-	-	22.9	1.197	22.6	0.516
80	90	0.8	31.8	0.789	-	-	27.5	1.080	27.6	0.516
81	90	0.9	40.1	2.132	-	-	34.6	0.843	36.3	1.160
82	100	0.1	6.6	0.516	-	-	5.0	0.000	5.0	0.000
83	100	0.2	10.1	0.568	-	-	7.5	0.527	7.9	0.316
84	100	0.3	13.0	0.471	-	-	11.1	0.316	10.2	0.422
85	100	0.4	16.5	0.850	-	-	14.5	0.850	13.2	0.422
86	100	0.5	19.9	0.738	-	-	18.4	0.699	16.2	0.422
87	100	0.6	24.1	0.568	-	-	22.5	0.707	19.9	0.568
88	100	0.7	28.5	1.269	-	-	27.0	1.054	24.2	0.632
89	100	0.8	35.1	1.370	-	-	32.7	1.337	30.5	0.850
90	100	0.9	44.3	1.703	-	-	38.1	0.738	40.2	0.919

Average number of colors
(lower is better)

Time to solution

TABLE VI: Mean time to solution (seconds) depends on number of nodes (N_V) and edge probability (p) for open source solver GLPK, Gurobi and quantum inspired SimCIM. The best result in average number of colors and time to solution is highlighted in bold.

	N_V	p	GLPK		Gurobi		SimCIM	
			mean	std	mean	std	mean	std
1	10	0.1	0.001	0.001	0.001	0.000	0.198	0.056
2	10	0.2	0.002	0.000	0.001	0.000	0.232	0.007
3	10	0.3	0.003	0.002	0.001	0.000	0.238	0.015
4	10	0.4	0.007	0.004	0.001	0.000	0.229	0.021

5	10	0.5	0.012	0.006	0.001	0.000	0.222	0.011
6	10	0.6	0.032	0.022	0.002	0.000	0.239	0.022
7	10	0.7	0.080	0.073	0.002	0.001	0.265	0.044
8	10	0.8	1.907	4.984	0.002	0.001	0.325	0.121
9	10	0.9	13.901	24.658	0.003	0.002	0.371	0.041
10	20	0.1	0.006	0.001	0.002	0.000	0.254	0.005
11	20	0.2	0.034	0.029	0.003	0.001	0.296	0.038
12	20	0.3	0.192	0.306	0.006	0.001	0.346	0.026
13	20	0.4	0.875	0.390	0.012	0.007	0.440	0.015
14	20	0.5	10.721	12.125	0.019	0.013	0.498	0.047
15	20	0.6	124.385	91.853	0.023	0.012	0.591	0.034
16	20	0.7	199.375	115.200	0.034	0.015	0.667	0.060
17	20	0.8	300.065	0.010	0.034	0.018	0.840	0.061
18	20	0.9	300.094	0.015	0.040	0.014	1.056	0.063
19	30	0.1	0.019	0.008	0.006	0.003	1.720	0.035
20	30	0.2	0.340	0.282	0.015	0.010	2.427	0.036
21	30	0.3	9.814	4.160	0.035	0.012	3.181	0.054
22	30	0.4	267.903	70.468	0.070	0.024	3.985	0.049
23	30	0.5	300.103	0.012	0.138	0.083	5.017	0.331
24	30	0.6	300.186	0.038	0.163	0.040	6.124	0.287
25	30	0.7	300.254	0.042	0.173	0.054	7.397	0.534
26	30	0.8	300.403	0.057	0.189	0.077	9.811	0.697
27	30	0.9	300.556	0.122	0.304	0.111	12.687	1.312
28	40	0.1	-	-	0.021	0.009	2.366	0.267
29	40	0.2	-	-	0.067	0.038	3.753	0.340
30	40	0.3	-	-	0.191	0.104	5.472	0.367
31	40	0.4	-	-	0.753	0.932	6.545	0.542
32	40	0.5	-	-	0.867	0.631	8.526	0.695
33	40	0.6	-	-	1.306	1.014	10.350	0.448
34	40	0.7	-	-	1.557	2.098	13.801	2.007
35	40	0.8	-	-	1.162	0.431	17.844	1.989
36	40	0.9	-	-	1.155	0.159	24.713	3.280
37	50	0.1	-	-	0.027	0.014	3.607	0.053
38	50	0.2	-	-	0.333	0.245	5.174	0.192
39	50	0.3	-	-	4.990	5.810	7.463	0.453
40	50	0.4	-	-	4.757	4.187	9.495	0.510
41	50	0.5	-	-	7.071	4.687	14.036	1.771
42	50	0.6	-	-	66.279	61.284	25.216	5.909
43	50	0.7	-	-	38.152	46.330	25.096	3.382
44	50	0.8	-	-	7.727	8.428	33.786	8.187
45	50	0.9	-	-	2.372	0.257	42.495	4.156
46	60	0.1	-	-	0.129	0.087	4.421	0.129
47	60	0.2	-	-	0.872	1.026	7.734	1.722
48	60	0.3	-	-	16.930	11.034	11.445	1.823
49	60	0.4	-	-	51.511	82.086	18.106	4.262
50	60	0.5	-	-	68.744	68.795	21.368	3.984
51	60	0.6	-	-	95.411	88.234	48.351	13.262
52	60	0.7	-	-	66.161	44.420	40.763	11.270
53	60	0.8	-	-	42.528	68.171	56.013	10.085
54	60	0.9	-	-	7.724	1.407	72.302	7.284
55	70	0.1	-	-	0.461	0.291	6.458	1.655
56	70	0.2	-	-	4.822	4.982	9.977	1.664
57	70	0.3	-	-	28.828	14.424	15.687	2.101
58	70	0.4	-	-	78.486	63.512	38.800	14.893
59	70	0.5	-	-	114.880	70.768	38.288	14.127
60	70	0.6	-	-	103.728	71.210	54.067	11.507
61	70	0.7	-	-	133.313	72.464	63.095	10.184
62	70	0.8	-	-	110.066	77.881	96.272	17.250
63	70	0.9	-	-	19.536	4.820	134.355	28.658
64	80	0.1	-	-	1.309	1.599	7.324	0.592
65	80	0.2	-	-	52.218	78.163	15.138	2.710

66	80	0.3	-	-	67.343	36.356	26.198	6.943
67	80	0.4	-	-	116.747	111.805	37.085	9.220
68	80	0.5	-	-	96.057	37.923	49.570	7.162
69	80	0.6	-	-	167.210	66.138	159.555	81.808
70	80	0.7	-	-	202.061	65.897	112.915	18.953
71	80	0.8	-	-	162.988	45.676	167.062	37.764
72	80	0.9	-	-	53.323	18.095	227.224	50.657
73	90	0.1	-	-	1.058	1.224	9.336	0.726
74	90	0.2	-	-	34.024	38.601	18.623	3.323
75	90	0.3	-	-	162.527	97.995	32.050	9.461
76	90	0.4	-	-	143.790	114.855	48.503	4.782
77	90	0.5	-	-	167.725	63.551	67.405	14.039
78	90	0.6	-	-	157.333	100.262	81.155	17.398
79	90	0.7	-	-	252.613	37.275	90.603	16.960
80	90	0.8	-	-	258.383	18.204	141.974	29.896
81	90	0.9	-	-	120.630	47.417	219.341	43.442
82	100	0.1	-	-	1.571	0.714	11.952	2.225
83	100	0.2	-	-	90.416	70.264	23.365	2.986
84	100	0.3	-	-	106.807	100.061	48.057	10.612
85	100	0.4	-	-	127.184	107.183	60.967	10.674
86	100	0.5	-	-	92.338	108.744	112.470	12.526
87	100	0.6	-	-	171.188	79.565	105.843	17.305
88	100	0.7	-	-	138.741	106.281	155.752	41.929
89	100	0.8	-	-	184.035	128.311	214.694	59.357
90	100	0.9	-	-	233.650	54.277	281.240	33.966
